Advances in Science and Technology Research Journal

Advances in Science and Technology Research Journal 2023, 17(4), 313–324
https://doi.org/10.12913/22998624/169573
ISSN 2299-8624, License CC-BY 4.0

Received: 2023.06.10
Accepted: 2023.07.17
Published: 2023.08.15

Bending Moment Control and Weight Optimization in Space Structures by Adding Extra Members in the Optimal locations

Ahmed Manguri[1,2*], Najmadeen Saeed[2,3], Marcin Szczepanski[1], Robert Jankowski[1]

[1] Faculty of Civil and Environmental Engineering, Gdansk University of Technology, Gdansk, Poland
[2] Civil Engineering Department, University of Raparin, Rania, Kurdistan Region, Iraq
[3] Civil Engineering Department, Faculty of Engineering, Tishk International University, Erbil, Iraq
* Corresponding author's e-mail: ahmed.manguri@pg.edu.pl

ABSTRACT

This paper investigates the reduction of bending moment in critical members by adding some extra members in the optimum location. Instead of enlarging the size of members to resist the moment, eight additional members are added in the optimum location to reduce the bending moment in the critical members. The total weight of the proposed structure with extra members is less than that of the original structure that resists the induced bending moment. Moreover, the location of the additional bars significantly reduces the nodal displacements. This paper investigates the effect of placing extra members on vertically and/or horizontally loaded egg-shaped single-layer frames. An egg-shaped structure is designed based on the maximum induced moment; in such frames, the bending moment is the dominant internal force. Then some extra members are suggested to be added to the structure to reduce the maximum bending moment to the lowest possible value; thus, the designed cross-sectional area is minimized. Furthermore, the optimized structure's total weight and shape deformation is less than the ordinary structure's. The study results show that the extra bars' location depends on the loadings' direction. Moreover, the weight of the horizontally loaded egg-shaped structure can be optimized by up to 28%. The results were verified by MATLAB and SAP2000 software.

Keywords: size optimization, weight optimization, additional bars, bending moment control, egg-shaped structure

INTRODUCTION

In the modern world, space structures have a large free column span and a low weight ratio to the covered area. Other purposes of building such systems are their aesthetic view and use as a storage [1]. Space structures can be found in several tourist cities, such as Pavilion and Science Museum (Nur Alem) in Kazakhstan [2, 3], MSG Sphere in Las Vegas in the US [4], and Ericsson Globe in Stockholm, Sweden [5, 6]. Due to loadings, the structural shape can be disturbed, and the internal bending moment, torsion, and axial forces can pass the allowable limits.

In general, the bending moment is the critical internal force in moment frames that causes noticeable deformation and sometimes failure in frame structures [7, 8]. Chen and Lui [9] discussed the types of space frames and several analysis methods. Researchers used different methods to analyze space frames, for example, the modified arch length method [10], Euler's finite rotation formula [11], and the stiffness matrix method [12]. Regarding minimizing bending moments in simple frames, Wang [13] suggested a computational technique to reduce flexural moments in frame members. Moreover, the shape disturbance of some types of space structures was reformed after deformation, for instance, double-layer domes [14, 15] and egg-shaped single-layer frames [16]. Moreover, the internal bar force is also reduced in the members with high-stress levels by prestressing some active members [17].

Finding the optimum solution for a given problem is essential for cost-effectiveness. Structural optimization opened a new chapter in structural engineering [18]. Structural optimization is defined as the process of finding the best solution for a particular concern [19-21] in systems. Bar size optimization was performed for truss [22-28], dome [29-31], and frame [32, 33] structures. Furthermore, the optimum location of different types of shear walls for various buildings [34] on several soil types [35] was investigated. The optimal design was done for I- and H-shaped crane bridge girders [36], reinforced concrete sections [37], and steel moment frames [38]. Moreover, the significance of the most active members' location to change the bars' lengths to reshape and redistribute stress in members was also studied [39-43]. So far, studies have not been carried out either to control bending moment in beams or to beam size optimization for space frames.

Moreover, Saeed et al. [16] added extra members to a single-layer egg-shaped frame; they were not interested in finding the best places for the extra bars to reduce the structural deformation and bar internal forces. They arbitrarily put eight members in two different places to change the length of the additional bars to minimize the deformed shape without regard to the bending moments and axial forces. So far, the significance of the location of additional bars on a frame has not been studied. This paper deals with adding extra bars in different places of two numerical models of a single-layer egg-shaped frame. One of the structures is hinged support, and the other is fixed support. The optimum location of the extra bars is determined based on the shape disturbance and structural stability. Aside from the original shape (Case 0), ten cases are evaluated; for each case, the extra members are added to different frame levels.

METHODS

Numerical modeling

The numerical model is 5000 mm high and 4000 mm wide. The model is formed by eleven circles of eight joints on top of each other. In addition to two joints, one at the very top and the other at the very bottom of the structure (Fig. 1a). Moreover, the numerical model is supported at the nine bottom joints. The ninety joints were connected with 176 bars, as illustrated in Figure 1b. The members are made of steel, with Young's modulus of 200 GPa; the bars' diameter depends on the members' maximum bending moment.

Eight members are attached to different levels of the structure to investigate the effect of the added members on the end moments and nodal displacements. For example, maximum absolute moment about the X-axis (max(abs(mx1)) max(abs(mx2))), the Y-axis (max(abs(my1)) max(abs(my2))). maximum absolute nodal displacements in X-direction (max(abs(dx)), Y-directions (max(abs(dy))), and Z-direction (max(abs(dz)))).

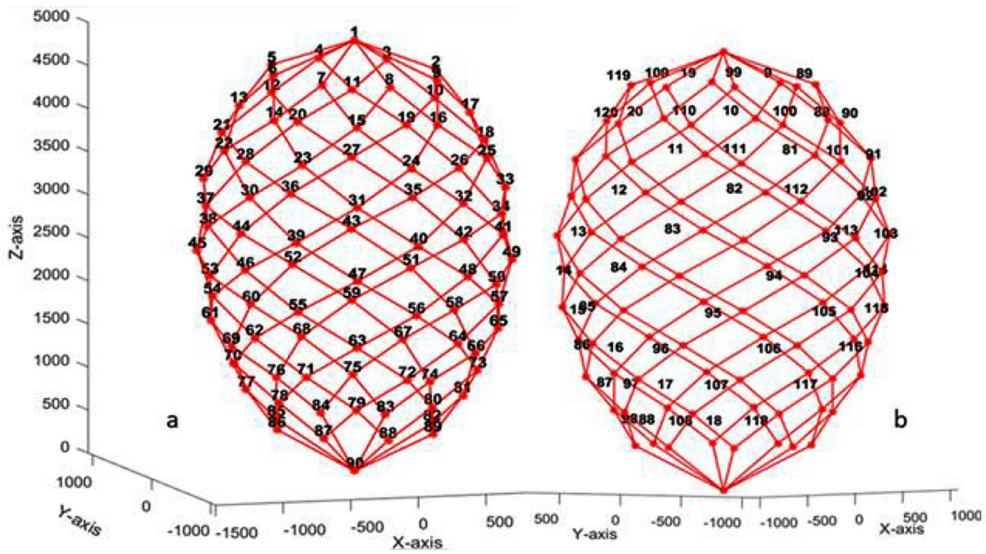

Figure 1. Single-layer egg-shaped frame: (a) joint labeling, and (b) member labeling

Optimization calculation

The area of the bars is selected based on the maximum moment in members, and the shape modulus is found as presented in Equation (1):

$$sx_i = M_{\max i} / fy \tag{1}$$

where: i is the case number, sx is the required shape modules, $M_{\max i}$ is the yield moment, and fy is the materials yield strength.

$$D_i = 2Iy / sx \tag{2}$$

where: D_i is the required bar's diameter to resist the maximum moment, and Iy is the moment of inertia.

The area and the volume for each case is calculated as Equations 3 and 4:

$$A_i = \frac{\pi}{4} D_i^2 \tag{3}$$

where: A_i is the required area for each case based on the maximum bending moment.

$$W_i = A_i * sum(L) * \gamma \tag{4}$$

where: W_i is the total weight of the structure bars for each case, and sum (L) is the summation of the length of the bars, and γ is the density of the material which 25 kN/m^3.

It should be noted that the $sum(L)$ of case 0 is less than that of the other cases since, for Case 0, there are no additional members. The optimization in the cross-sectional area and the total volume is based on Equations 5 and 6:

$$Opt_{area} = \frac{A_0 - A_i}{A_0} * 100 \tag{5}$$

$$Opt_{vol} = \frac{W_0 - W_i}{W_0} * 100 \tag{6}$$

RESULTS AND DISCUSSION

This section studies the significance of extra members' locations. Aside from the original shape (case 0), ten other cases are evaluated. For each case, the additional members are added in different levels of the frame. Since the number of joints in each level is eight, the extra member's number for each case is eight bars. In other words, the additional members are horizontal and connect the eight joints in ten various levels, as presented in Figure 2.

Horizontal loading

Two loading cases are investigated to understand the structure's behavior for different horizontal loadings cases.

Loading Joints 18-21

In this loading case, joints 18-21 are loaded horizontally with 60N. The maximum induced

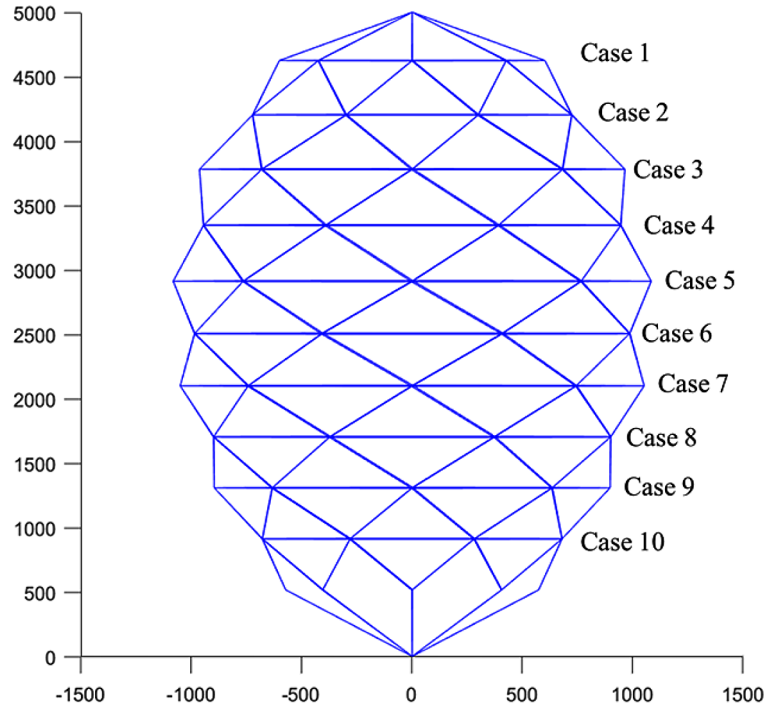

Figure 2. Optimization of cross-sectional area and total volume of the structure in eleven cases

bending moments for the original structure (Case 0) and the ten cases are illustrated in Figure 2. According to the data presented in Figure 3, the optimum location for placing the extra members for the given loading case is Case 9. Numerically speaking, the maximum bending moment for Case 9 is 9077 N·mm, while the maximum induced bending moment for Case 0 is 16249 N·mm. The optimization of beam cross-sectional area and material expenditure is illustrated in Figure 4. In terms of nodal displacements, the joints of the structure of Case 0 face larger movements than that of Case 9 (see Figure 5). This is because the bending moment is the substantial factor of deformation in moment frames. Furthermore, the bending moment in members for Case 0 is larger than that for Case 9, as presented in Figure 6.

Loading Joints 26-29

In this case, Joints 26-29 are loaded horizontally to see if still Case 9 is the optimum case. By changing the loading position, the amount of bending moment is changed; however, Case 9 is still the best-case scenario. Figure 7 shows the maximum absolute bending moments for eleven cases, including the original case (Case 0). It can be seen that the maximum induced moment for cases 0 and 9 is 13262 N·mm and 5543 N·mm, respectively. Based on the maximum bending moments, the optimization of the cross-sectional

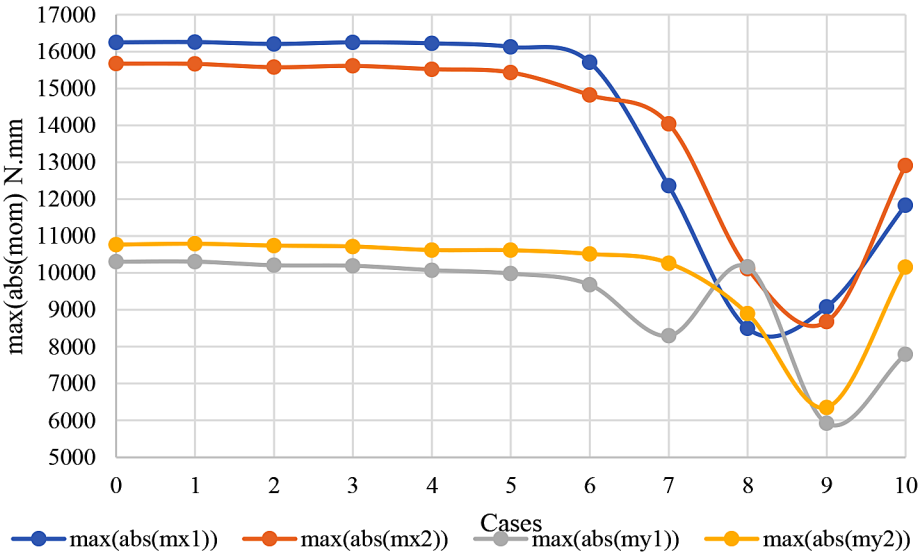

Figure 3. Maximum absolute bending moments for eleven cases

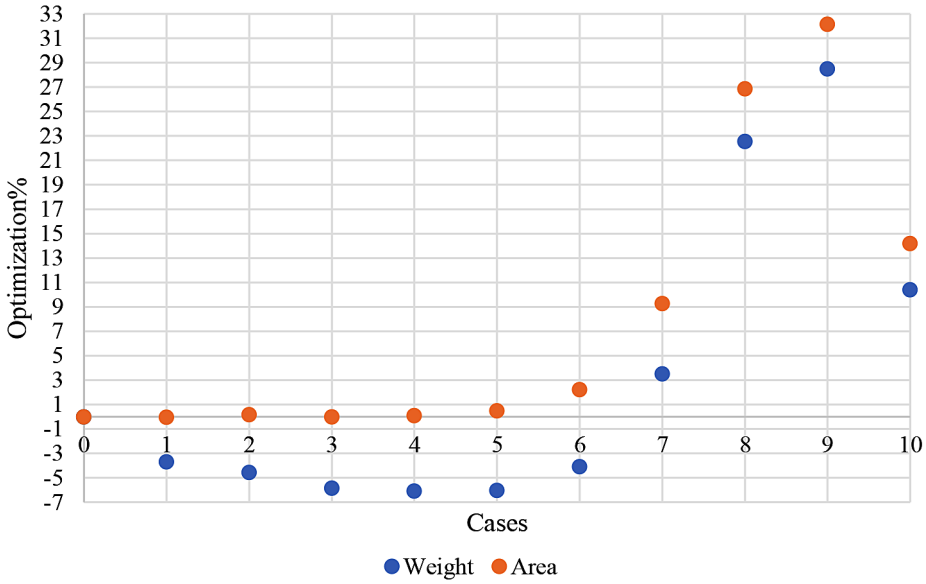

Figure 4. Optimization of cross-sectional area and the total weight of the structure in eleven cases

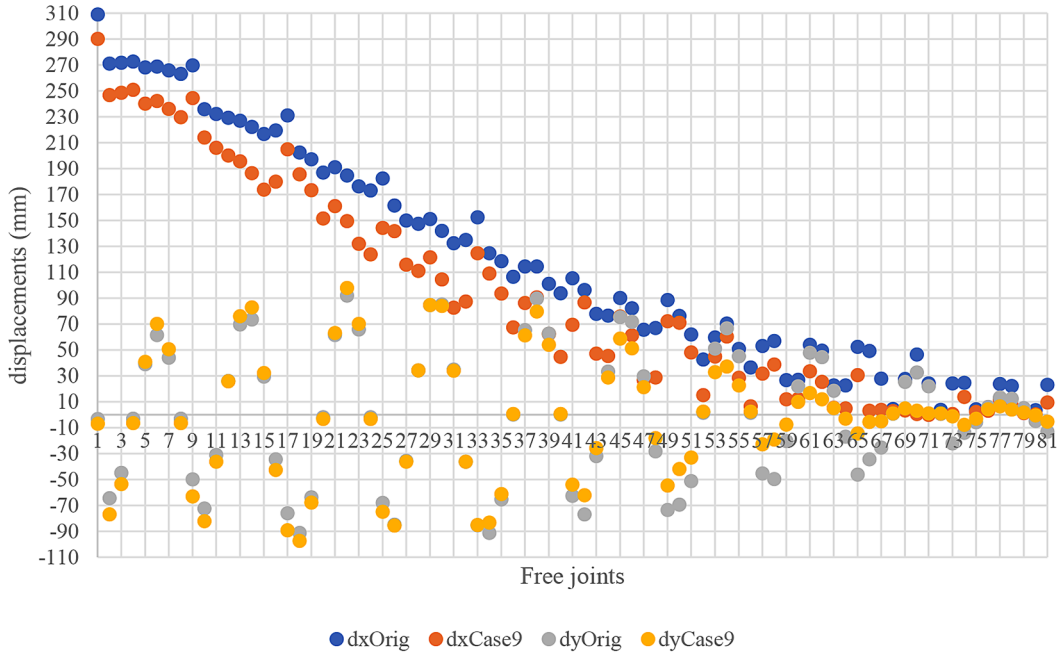

Figure 5. Nodal displacements of Case 0 and 9 in X and Y directions

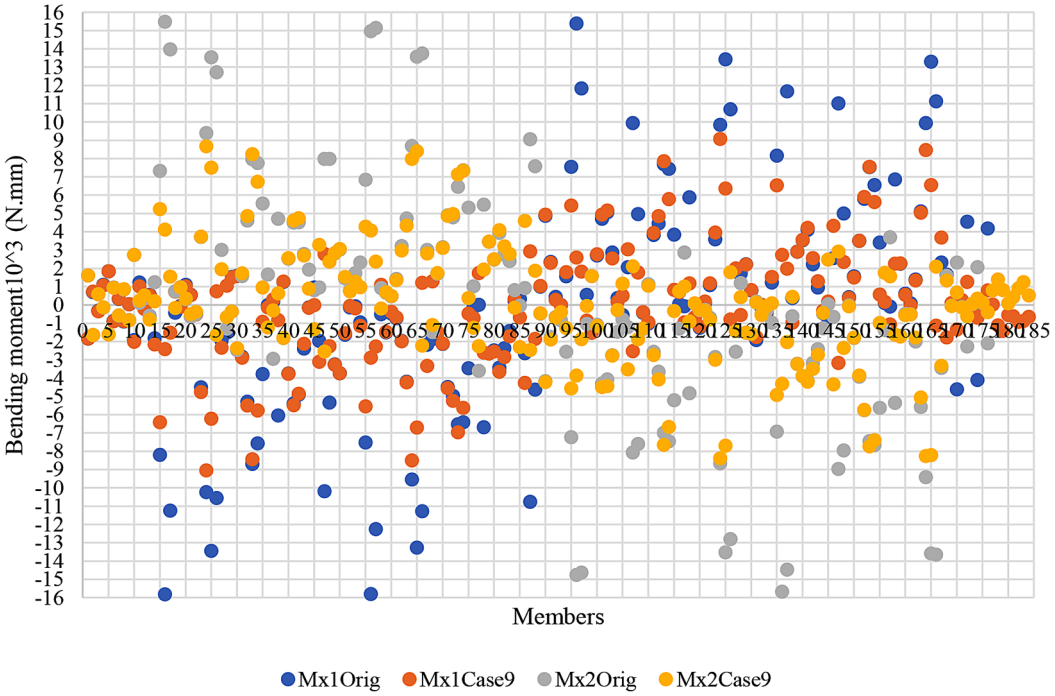

Figure 6. Bending moments in members about the X axis for Cases 0 and 9

bar area and the total weight of the structure is presented in Figure 8. The figure shows that the optimization of the cross-sectional area and the total weight of Case 9 based on the original case is 25% and 20% respectively.

Vertical loading

This section studies two different cases of vertical loadings to investigate the effect of loading in bending moments and the place of additional members.

Loading Joints 1, 10-17

In this case, joints 1, 10-17 are loaded vertically with 180 N downward. The induced flexural moment in eleven cases is presented in Figure 9. The figure shows that the best-case scenario is Case 6, which provides with least bending moments. Case

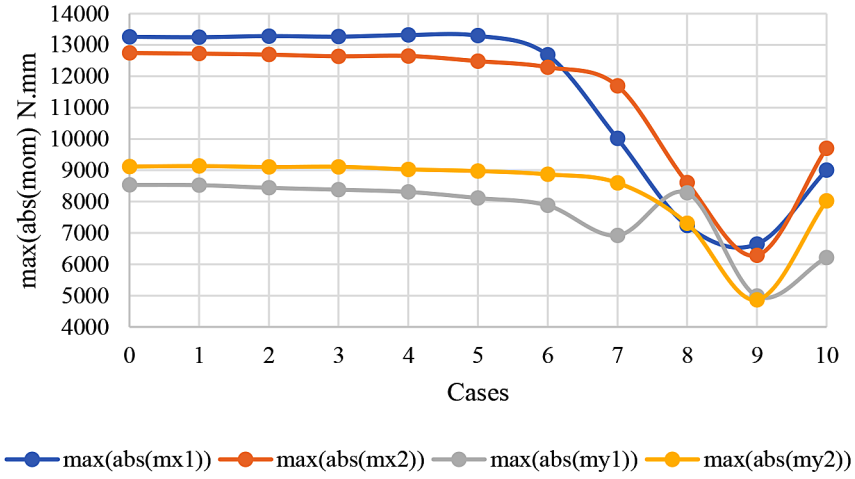

Figure 7. Maximum absolute bending moments for eleven cases

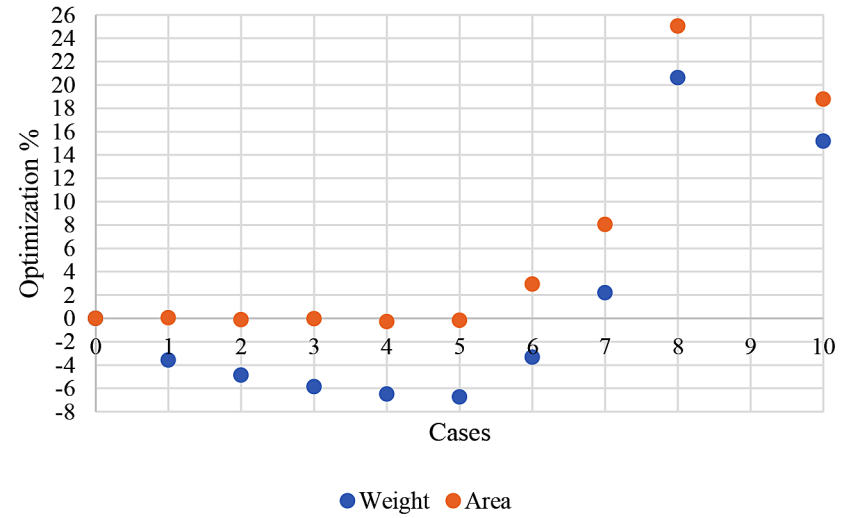

Figure 8. Optimization of cross-sectional area and total weight of the structure in eleven cases

6 provides bar size and structural total weight by 12 and 6%, respectively, as illustrated in Figure 10. Moreover, the states of the nodal displacements in X and Y directions of the optimal case (Case 6) and the original structure (Case 0) is presented in Figure 11. Despite of smaller size of beams in case 6 compared to case 0, the nodal displacements of case 6 are smaller than that of case 0. Similarly, the states of bending moments of all members about the X-axis for the optimal case and the original structure are illustrated in Figure 12. The figure shows that the induced bending moments in members for Case 0 are more prominent than that in case 6.

Loading Joints 1, 18-25

In this case, joints 1, 18-25 are loaded vertically with 180 N downward. The purpose of changing the loading joints is to see the behavior of the structure in eleven cases. Figure 13 shows the induced bending moments in all cases, and one can see that still Case 6 is the best-case scenario. Figure 14 shows the structure's optimization in area and weight in Cases 1-10 based on Case 0. However, the beam cross-sectional area is minimized in Cases 5, 6, and 7, the total weight of Cases 5 and 7 is greater than that of Case 0. This is because Case 0 has only 176 beams, while other cases have 174 (176+8) beams. Moreover, the total weight optimization of Case 6 is just under 4%.

Horizontal and vertical loading simultaneously

In this loading case, Joints 1 to 9 are loaded vertically with -180 N, and joints 18-21 are loaded horizontally with 60 N. The induced bending moments in eleven cases are illustrated in Figure 15.

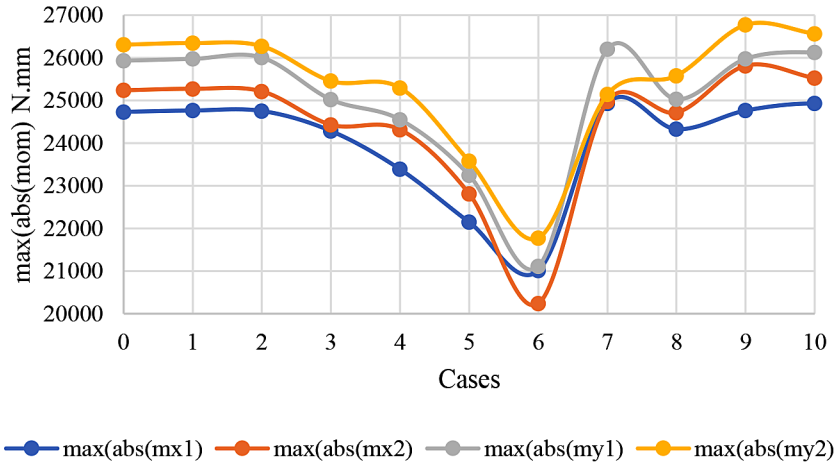

Figure 9. The maximum absolute bending moments of the egg-shaped single layer in eleven cases

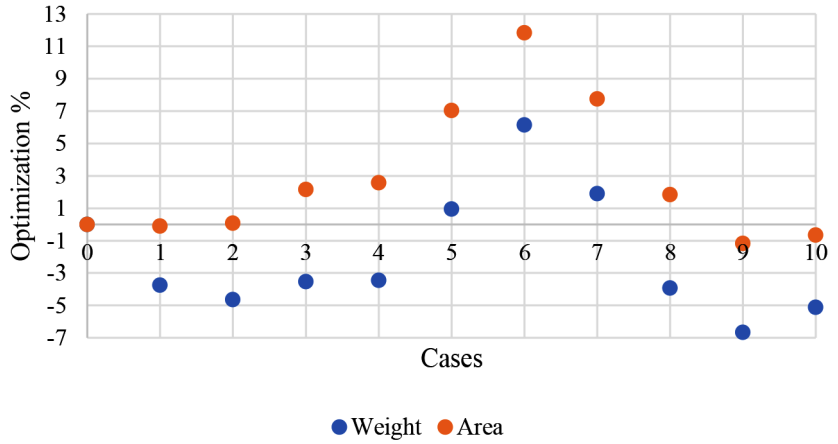

Figure 10. Optimization of bar size and weight in eleven cases

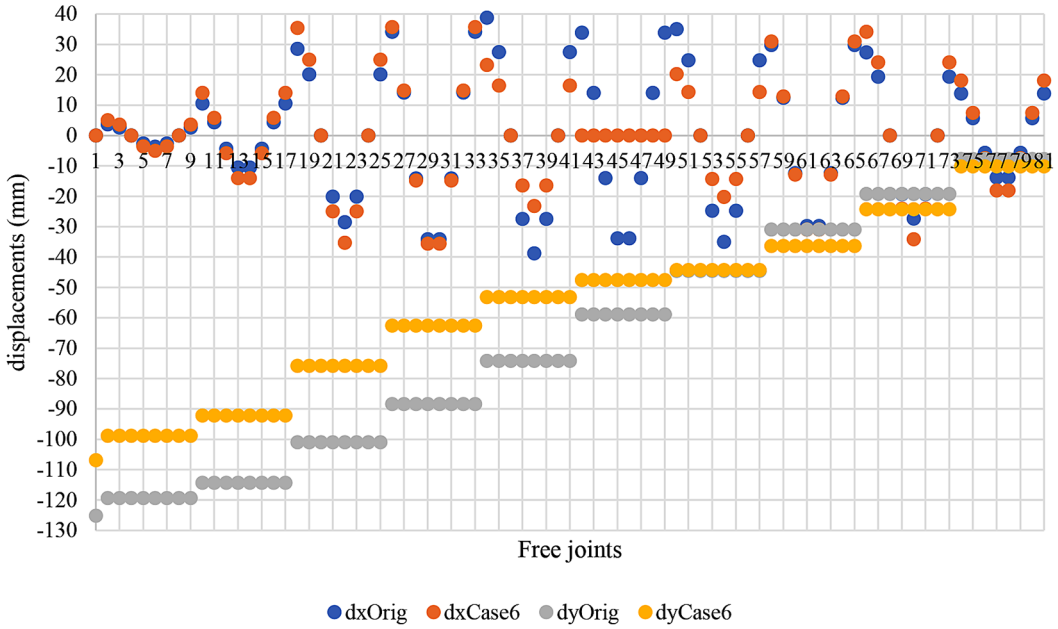

Figure 11. X and Y displacements of nodes for Cases 0 and 6

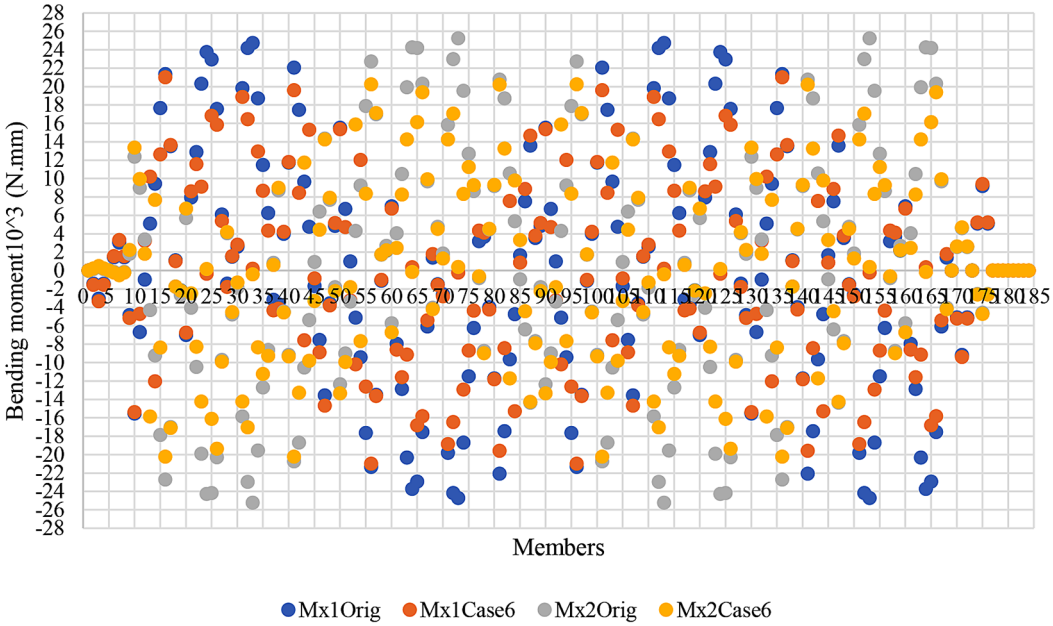

Figure 12. The states of bending moments in members for cases 0 and 6

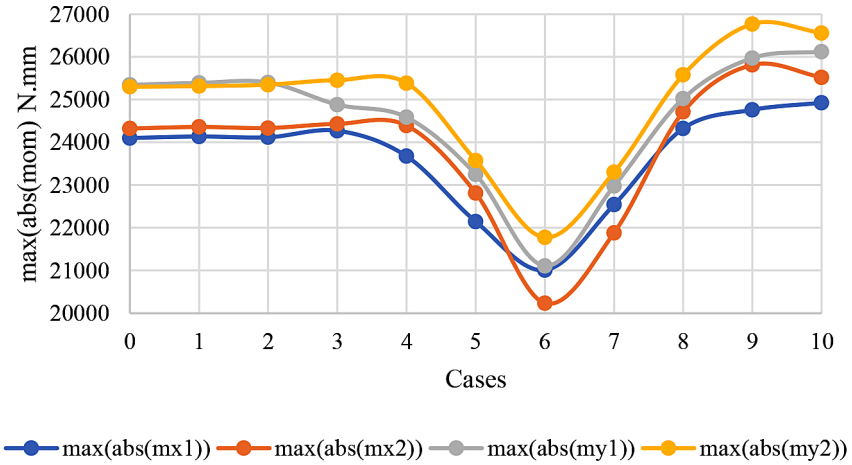

Figure 13. Maximum bending moments in eleven cases

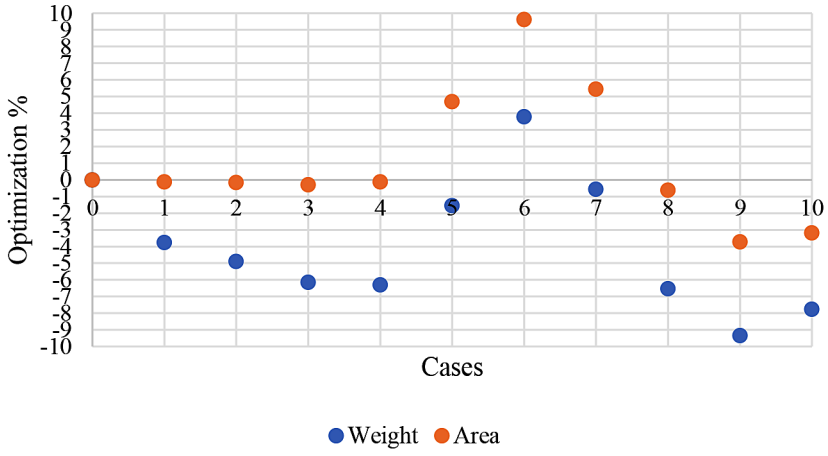

Figure 14. Cross-sectional area and weight optimization of ten cases compared to Case 0

One can see that the best case scenario is case 7, with the maximum bending moment of 30597 N.mm. Regarding the bar size and weight optimization, Figure 16 shows that the beam size and weight optimization of case 7 are 14% and 8.5%, respectively. Regarding nodal displacements, the movements of the optimum case are smaller than that of the original case (Fig. 17). Furthermore, the states of the bending moments of each member for Cases 0 and 7 are illustrated in Figure 18. One can see that the optimum case's bending moments are more miniature than Case 0.

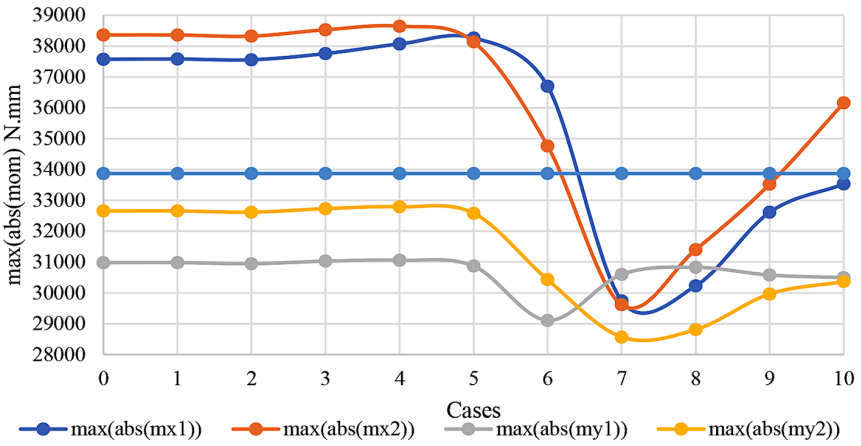

Figure 15. Maximum bending moments for eleven cases

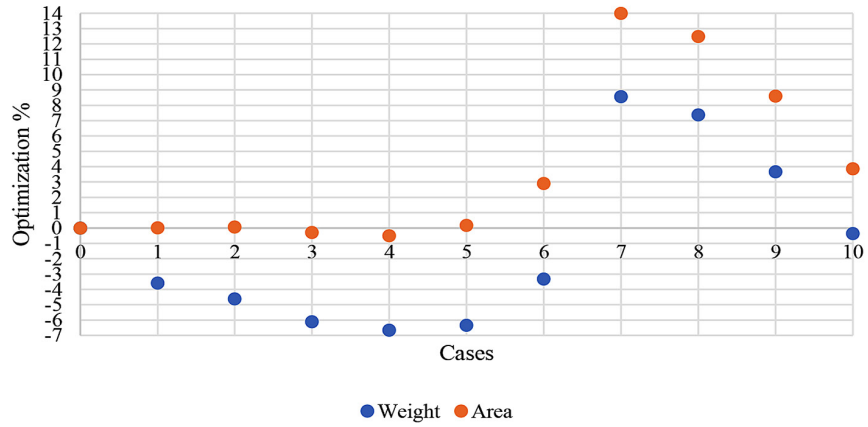

Figure 16. Cross-sectional are and weight optimization for X and Y loading case

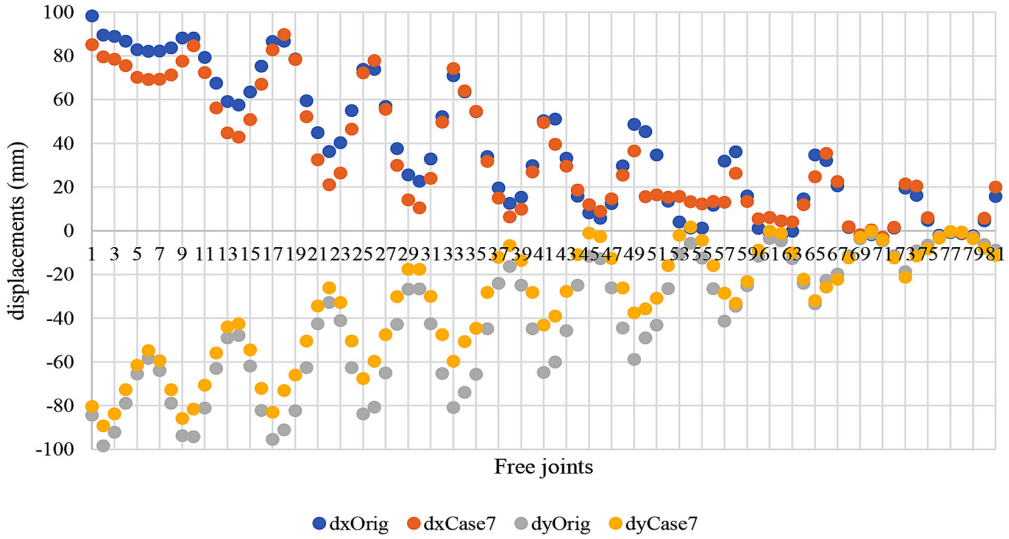

Figure 17. Nodal displacements for the optimum cases and the original structure

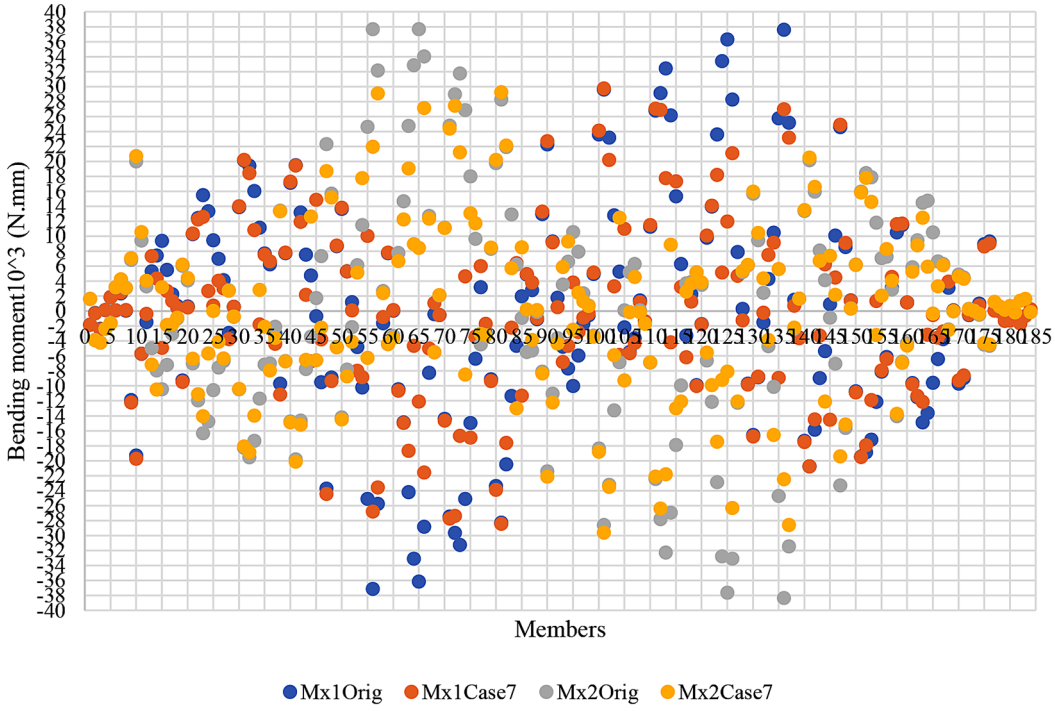

Figure 18. Bending moments in all members for Cases 0 and 7

CONCLUSION

In this study, the total structural weight of a space frame has been minimized; in addition, the significance of the location of the additional bars on the behavior of single-layer egg-shaped frames in several loading cases was investigated. The effectiveness of the location of the redundant on bending moment, beam size and total weight of the structure, and deformation of the structure has been extensively discussed. It was found that the place of the redundant is significant in the behaviors of the structure. The optimum location of the extra members depends on the loadings' direction. The structure's total weight optimization can be obtained up to 28%, 6%, and 8.5% for horizontally, vertically, and simultaneously horizontally and vertically loaded structures, respectively.

REFERENCES

1. Sutter, G. and Jäger, P., Egg-shaped anaerobic digesters, Taiwan. Structural Engineering International, 1994; 4(3): 160-163. https://doi.org/10.2749/101686694780601999
2. Winterstetter, T., et al., Innovative Bautechnik im Herzen Asiens–die EXPO 2017 in Astana, Kasachstan. ce/papers, 2018; 2(1): 51-57. https://doi.org/10.1002/cepa.630
3. Bechmann, R., et al., Eine runde Sache: Stahl-Glas-Tragwerke für die EXPO 2017 in Astana. Stahlbau, 2019; 88(1): 57-63. https://doi.org/10.1002/stab.201800022
4. Richard, B., Las Vegas: past, present and future. Journal of Tourism Futures, 2018.
5. Chang, X. and Haiyan, X. Using sphere parameters to detect construction quality of spherical buildings. in 2nd International Conference on Advanced Computer Control. Shenyang, China, 2010 https://doi.org/10.1109/ICACC.2010.5487073
6. Manguri, A., et al., Optimal reshaping and stress control of double-layer spherical structures under vertical loadings. Archives of Civil Engineering, 2022; 68(4). https://doi.org/10.24425/ace.2022.143056
7. Gordo, J. and Soares, C.G., Experimental analysis of the effect of frame spacing variation on the ultimate bending moment of box girders. Marine Structures, 2014; 37: 111-134. https://doi.org/10.1016/j.marstruc.2014.03.003
8. Bai, Y., Shi, Y., and Deng, K., Collapse analysis of high-rise steel moment frames incorporating deterioration effects of column axial force–bending moment interaction. Engineering Structures, 2016; 127: 402-415. https://doi.org/10.1016/j.engstruct.2016.09.005
9. Chen, W.F. and Lui, E.M., Handbook of structural engineering. CRC press, 2005.
10. Meek, J. and Tan, H.S., Geometrically nonlinear analysis of space frames by an incremental iterative technique. Computer methods in applied mechanics

engineering Structures, 1984; 47(3): 261-282. https://doi.org/10.1016/0045-7825(84)90079-3

11. Correia, A.A. and Virtuoso, F.B. Nonlinear analysis of space frames. in III European Conference on Computational Mechanics. 2006 107-107. https://doi.org/10.1007/1-4020-5370-3_107
12. Saeed, N., et al., Non-Linear Analysis of Structures Utilizing Load-Discretization of Stiffness Matrix Method with Coordinate Update. Applied Sciences, 2022; 12(5): 2394.
13. Wang, D., Optimal shape design of a frame structure for minimization of maximum bending moment. Engineering structures, 2007; 29(8): 1824-1832. https://doi.org/10.1016/j.engstruct.2006.10.004
14. Manguri, A., Saeed, N., and Haydar, B. Optimal Shape Refurbishment of Distorted Dome Structure with Safeguarding of Member Stress. in 7th International Engineering Conference "Research & Innovation amid Global Pandemic"(IEC). Erbil, Iraq, 2021 90-95. https://doi.org/10.1109/IEC52205.2021.9476107
15. Saeed, N., Manguri, A., and Al-Zahawi, S. Optimum Geometry and stress control of deformed double layer dome for gravity and lateral loads. In: 7th International Engineering Conference Research & Innovation amid Global Pandemic (IEC). Erbil, Iraq, 2021, 84-89. https://doi.org/10.1109/IEC52205.2021.9476094
16. Saeed, N., et al. Shape restoration of deformed egg-shaped single layer space frames. In: International Conference on Advanced Science and Engineering (ICOASE). Duhok, Kurdistan Region, Iraq, 2019, 220-225. http://dx.doi.org/10.1109/ICOASE.2019.8723714
17. Kwan, A. and Pellegrino, S., Prestressing a space structure. AIAA journal, 1993; 31(10): 1961-1963. https://doi.org/10.2514/3.11876
18. Kaveh, A., Optimal structural analysis. John Wiley & Sons, 2014.
19. Christensen, P.W. and Klarbring, A., An introduction to structural optimization. Vol. 153. Springer Science & Business Media, 2008.
20. Spillers, W.R. and MacBain, K.M., Structural optimization. Springer Science & Business Media, 2009.
21. Haftka, R.T. and Gürdal, Z., Elements of structural optimization. Vol. 11. Springer Science & Business Media, 2012.
22. Mai, H.T., et al., A novel deep unsupervised learning-based framework for optimization of truss structures. Engineering with Computers, 2022: 1-24. https://doi.org/10.1007/s00366-022-01636-3
23. Nguyen-Van, S., et al., A novel hybrid differential evolution and symbiotic organisms search algorithm for size and shape optimization of truss structures under multiple frequency constraints. Expert Systems with Applications, 2021; 184: 115534. https://doi.org/10.1016/j.eswa.2021.115534
24. Lewiński, T., et al., Topology optimization in structural mechanics. Bulletin of the Polish Academy of Sciences: Technical Sciences, 2013; (1).
25. Nowak, M. and Boguszewski, A., Topology optimization without volume constraint–the new paradigm for lightweight design. Bulletin of the Polish Academy of Sciences: Technical Sciences, 2021.
26. Manguri, A., et al., Optimum number of actuators to minimize the cross-sectional area of prestressable cable and truss structures. Structures, 2023; 47: 2501-2514. https://doi.org/10.1016/j.istruc.2022.12.031
27. Bojczuk, D. and Rębosz-Kurdek, A., Topology optimization of trusses using bars exchange method. Bulletin of the Polish Academy of Sciences. Technical Sciences, 2012; 60(2): 185-189.
28. Brütting, J., Senatore, G., and Fivet, C., MILP-based discrete sizing and topology optimization of truss structures: new formulation and benchmarking. Structural and Multidisciplinary Optimization, 2022; 65(10): 277. 10.1007/s00158-022-03325-7
29. Carvalho, J.P., et al., Simultaneous sizing, shape, and layout optimization and automatic member grouping of dome structures. Structures, 2020; 28: 2188-2202. https://doi.org/10.1016/j.istruc.2020.10.016
30. Kaveh, A. and Ilchi Ghazaan, M., Optimal seismic design of 3D steel frames, in meta-heuristic algorithms for optimal design of real-size structures. 2018, Springer. p. 139-155.
31. Kaveh, A. and Ilchi Ghazaan, M., Optimal Design of Dome-Shaped Trusses, in Meta-heuristic Algorithms for Optimal Design of Real-Size Structures. 2018, Springer. p. 101-122.
32. Mojtabaei, S.M., Becque, J., and Hajirasouliha, I., Structural size optimization of single and built-up cold-formed steel beam-column members. Journal of Structural Engineering, 2021; 147(4).
33. Peng, B., et al., Cost-based optimization of steel frame member sizing and connection type using dimension increasing search. Optimization Engineering Structures, 2022; 23(3): 1525-1558. https://doi.org/10.1007/s11081-021-09665-5
34. Krishna, M. and Arunakanthi, D.E., Optimum location of different shapes of shear walls in unsymmetrical high rise buildings. International Journal of Engineering Research Technology, 2014; 3(9): 1099-1106.
35. Al-Askari, A.N.A. and Rao, N.R., Study on the optimum location and type of shear wall in u-shape building under different types of soils. International Journal of Scientific Engineering and Technology Research, 2014.
36. Alhorani, R.A., Mathematical models for the optimal design of I-and H-shaped crane bridge girders. Asian

Journal of Civil Engineering, 2020; 21(4): 707-722. https://doi.org/10.1007/s42107-020-00232-4

37. Jha, B.K. and Bhanja, S., Optimum design of reinforced concrete sections in flexure and shortcomings of prescriptive method of design. Asian Journal of Civil Engineering, 2021; 22(4): 769-787. https://doi.org/10.1007/s42107-020-00346-9
38. Shahrouzi, M. and Farah-Abadi, H., Optimal seismic design of steel moment frames by un-damped multi-objective vibrating particles system. Asian Journal of Civil Engineering, 2018; 19(7): 877-891. https://doi.org/10.1007/s42107-018-0070-z
39. Yuan, S. and Jing, W., Optimal Shape Adjustment of Large High-Precision Cable Network Structures. AIAA Journal, 2021; 59(4): 1441-1456. https://doi.org/10.2514/1.J059989
40. Saeed, N.M., Manguri, A.A.H., and Adabar, A.M., Shape and force control of cable structures with minimal actuators and actuation. International Journal of Space Structures, 2021; 36(3): 241-248. https://doi.org/10.1177/09560599211045851
41. Saeed, N.M., et al., Static Shape and Stress Control of Trusses with Optimum Time, Actuators and Actuation. International Journal of Civil Engineering, 2023; 21(3): 379-390. http://dx.doi.org/10.1007/s40999-022-00784-3
42. Saeed, N., et al., Using Minimum Actuators to Control Shape and Stress of a Double Layer Spherical Model Under Gravity and Lateral Loadings. Advances in Science and Technology Research Journal, 2022; 16(6): 1-13. 10.12913/22998624/155214
43. Manguri, A., et al., Buckling and shape control of prestressable trusses using optimum number of actuators. Scientific Reports, 2023; 13(1): 3838. http://dx.doi.org/10.1038/s41598-023-30274-y